



**Folic acid modified Copper oxide nanoparticles for targeted delivery in in vitro and in vivo system**

Journal:	<i>RSC Advances</i>
Manuscript ID:	RA-ART-05-2015-008110.R3
Article Type:	Paper
Date Submitted by the Author:	22-Jul-2015
Complete List of Authors:	Laha, Dipranjan; Jadavpur University, Life Science and Biotechnology Pramanik, Arindam; Jadavpur University, Life Science and Biotechnology Chattopadhyay, Sourav; Vidhyaysagar University, Department of Human Physiology with Community Health Dash, Sandeep; Vidhyaysagar University, Department of Human Physiology with Community Health Roy, Somenath; Vidhyaysagar University, Department of Human Physiology with Community Health Pramanik, Panchanan; Indian Institute of Technology, Department of Chemistry Karmakar, Parimal; Jadavpur University, Life Science and Biotechnology



## Journal Name

## ARTICLE

## Folic acid modified Copper oxide nanoparticles for targeted delivery in in vitro and in vivo system

Received 00th January 20xx, Dipranjan Laha<sup>a</sup>, Arindam Pramanik<sup>a</sup>, Sourav Chattopadhyay<sup>b</sup>, Sandip kumar Dash<sup>b</sup>, Somenath Roy<sup>b</sup>, Panchanan Pramanik<sup>c</sup>, Parimal Karmakar<sup>a\*</sup>

Accepted 00th January 20xx

DOI: 10.1039/x0xx00000x  
[www.rsc.org/](http://www.rsc.org/)

### Abstract

Copper oxide nanoparticles are known to exhibit toxic effects on a variety of cell types. In the present study—copper oxide nanoparticles were modified with folic acid for targeted delivery. The physiochemical properties of copper oxide nanoparticles (CuO NPs) and folic acid conjugated copper oxide nanoparticles (CuO-FA NPs) were studied by Dynamic light scattering (DLS), Field emission scanning electron microscopy (FE-SEM) and Fourier transform infrared spectroscopy (FTIR). To determine targeting efficacy, we have used folate receptor positive and folate receptor knock down human breast cancer cells MCF7 (FR<sup>+</sup> MCF7). Flow cytometric analysis, generation of ROS and expression of apoptotic proteins (cleaved PARP, decreased p-BAD) indicated that most of cell death occurred through apoptosis in CuO-FA NPs treated MCF7 cells. In the in vivo study, we used Dalton's lymphoma (DL) cells induced tumor in mice. We successfully delivered CuO and CuO-FA NPs through peritoneal injection after induction of tumor. Reactive oxygen species (ROS), Glutathione (GSH) was measured in DL cells isolated from tumor bearing mice. All of these data indicated that CuO-FA NPs was more effective to kill the tumor cells and successful reduction of tumor was observed in CuO-FA NPs treated mice after 15 days treatment. These findings have important implications for understanding the potential anticancer property induced by folic acid modified CuO NPs.

**Key words:** folic acid, copper oxide nanoparticles, reactive oxygen species, tumor, apoptosis

### 1. Introduction

Cancer is a great threat to public health with more than 3.2 million new cases being diagnosed and more than 1.7 million patients lose their lives each year. Among the several cancers, breast cancer is the

second most common cancer among women in India and accounts for 7% of global burden of breast cancer.<sup>1</sup> While during treatment most of the cancer patients are suffering from the toxicity and side effects of chemotherapeutic agents. Thus, the development of new drugs with high efficacy and high selectivity for cancer cells is becoming more and more important.

Recently, Nanotechnology is expected to have a revolutionary impact on biology and medicine.<sup>2</sup> Different aspects of nanomaterials that may interfere with toxicity (e.g. size, shape, solubility, aggregation and optical features) have been addressed.<sup>3,4</sup> Now a

<sup>a</sup>Dept. Of Life science and Biotechnology, Jadavpur University, Kolkata, 700032

<sup>b</sup>Immunology and Microbiology Laboratory, Department of Human Physiology with Community Health, Vidyasagar University, Midnapore-721 102, West Bengal, India.

<sup>c</sup>Department of Chemistry, Indian Institute of Technology, Kharagpur, India.

E-mail: [pkarmakar\\_28@yahoo.co.in](mailto:pkarmakar_28@yahoo.co.in); Fax: +9133-24137121; Tel: +91 33-24146710

days, metal based or specifically transition metal based nanoparticles have drawn a great interest due to their high redox cycling property and their capacity to exert cytotoxicity on different cells via oxidative stress.<sup>5</sup> Several studies focusing on metal oxide NPs have demonstrated that these nanoparticles have toxic effects in cells and organisms. For example, Titanium dioxide ( $\text{TiO}_2$ ) nanomaterials (NMs) induced toxicity in vitro and in vivo under normal conditions.<sup>6</sup> Kim et al also reported that the cytotoxic effects of differently charged  $\text{SiO}_2$  and  $\text{ZnO}$  nanoparticles, with mean sizes of either 100 or 20 nm respectively, on the U373MG human glioblastoma cell line.<sup>7</sup> Bucchianico et al also observed that the CuO NPs caused genotoxicity, mitochondrial dysfunction and increased cell death in different human cell lines.<sup>8</sup> Among the different transition metal based nanoparticles, the synthesis procedure and surface modification of copper oxide nanoparticles is easy and also cheap compare to other metal based nanoparticles. In our previous study, we also demonstrated the cytotoxic effect of some copper based nanoparticles on human breast cell line MCF7.<sup>9</sup>

Although, the cytotoxic effect of these metal based nanoparticles is suitable to kill cancer cells but they are equally toxic to normal cells, which leads severe side effects.<sup>10</sup> Even the most advanced chemotherapeutic agents do not differentiate between normal cells and cancerous cells efficiently, which leads to nonspecific distribution of drug in the body and causes systemic toxicity and adverse effects.<sup>11</sup> In order to achieve the desired therapeutic effect in the tumor tissue, large quantity of the drug has to be administered, but this is not economical and undesirable toxicity may also appear.

Recently, several researchers focused on the nanoparticles as a promising carrier system for the delivery of chemotherapeutic agents by using both active and passive targeting to avoid systemic toxicity or normal cell toxicity.<sup>4,12</sup> On the other hand, nanoparticles can be also used as therapeutic agents by proper targeting. Passive targeting can differentiate between normal and tumor tissues and has the advantage of direct permeation to tumor tissue. But active targeting needs several ligands, where corresponding receptors are over-expressed in cancer cells. Folate receptors have been found to over-express in different human cancers including kidney, breast, ovaries, brain etc. Moreover, folic acid has a high affinity for folate receptor on the cell surface and non-proliferating normal cells are restricted in possessing folate receptors which provide highly selective sites that differentiate tumor cells from normal cells.<sup>13,14</sup> Thus, the receptor for folic acid constitutes a useful target for delivery of drug to the cancer cells. Here, we have developed a targeted delivery system using folic acid as a targeting agent for the delivery of CuO NPs. We

used both in vitro and in vivo model to test the efficacy of such folic acid conjugated CuO NPs. In in vitro system, the cytotoxic effect of CuO NPs and FA modified CuO NPs (CuO-FA NPs) was tested on both folate receptor positive and folate receptor knock down breast cancer cell line MCF7. In vivo system, we treated CuO NPs and CuO-FA NPs in Dalton's lymphoma (DL) induced tumor in swiss albino mice. We have seen that CuO-FA NPs is more active in comparison to CuO NPs in MCF7 cells and also Dalton lymphoma (DL) tumor bearing in mice.

## 2. Result and Discussion

### 2.1 Physical characterization:

#### 2.1.1 Dynamic Light Scattering (DLS), Field Emission Scanning Electron Microscopy (FESEM)

The physical characterization of CuO NPs and CuO-FA NPs was done by DLS and FESEM. From the DLS study, it was observed that the hydrodynamic size of CuO NPs and CuO-FA NPs were  $349 \pm 24$  nm and  $402 \pm 31$  nm respectively (Fig. 1A, B). From the FESEM study, it was seen that the sizes of CuO and CuO-FA NPs were  $35 \pm 3$  nm and  $42 \pm 4$  nm respectively with almost spherical geometry (Fig. 1C, D).

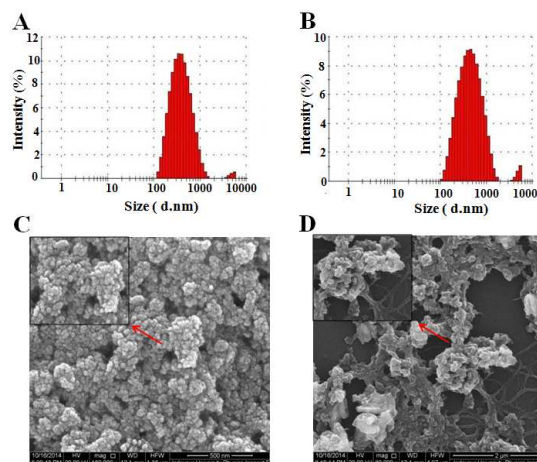


**Figure 1:** DLS study of (A) CuO NPs (B) CuO-FA NPs, FESEM image of (C) CuO NPs, (D) CuO-FA NPs respectively.

**Table 1.** Physical characterization of CuO NPs and CuO-FA NPs

PARTICLE	DLS Size (nm)	FESEM Size (nm)	Polydispersity Index
CuONPs	349±24	35±3	0.289
CuO-FA NPs	402±31	42±4	0.315

### 2.1.2 Fourier transform infrared spectroscopy study

FTIR spectroscopy is a useful tool to understand the functional group of any organic molecule. Conjugation of folic acid (FA) with CuO NPs was confirmed by FTIR study. Fig. 2 showed that the pure CuO NPs exhibit strong band at  $585\text{ cm}^{-1}$  characteristic of the Cu-O bond and broad band around  $3440\text{ cm}^{-1}$ , which indicates the presence of -OH groups on the nanoparticle's surface. The FTIR spectra of CuO-FA NPs showed two clear absorbance  $1132\text{ cm}^{-1}$  and  $1618\text{ cm}^{-1}$  which are similar absorbance peak present in FA. FTIR spectra of CuO-FA NPs indicated that the successful modification of FA molecules onto CuO NPs was mostly due to presence of amine group.

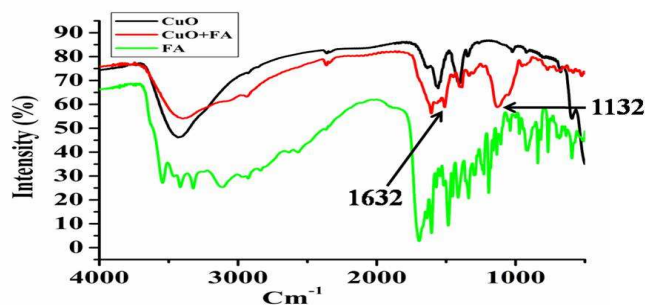


Figure 2: FTIR study of CuO NPs, FA+CuO NPs, FA

### 2.1.3 Zeta potential study

Zeta potential of CuO and CuO-FA NPs were measured at pH 7 to further verify the presence of folic acid on the nanoparticles. Zeta potential measurement showed that the surface zeta potential value of CuO and CuO-FA NPs are  $-38.4\text{ mV}$  and  $23.7\text{ mV}$  respectively. The positive raise in zeta potential value indicated that conjugation of FA on the surface of CuO NPs. This is due to the fact that negatively charged carboxyl group of FA easily conjugated with positively functionalized CuO NPs through amide bond formation. This phenomenon explained the proper modification of surface of CuO NPs by APTS followed by the attraction of the amine group of CuO NPs with carboxyl group of FA.

Table 2: Zeta potential value of CuO and CuO-FA NPs

PARTICLE	Zeta potential (mV)
CuO NPs	$-38.5 \pm 4.1$
CuO-FA NPs	$23.7 \pm 2.4$

### 2.2 Folate receptor (FR) expression

Knock down of folate receptor expression was determined by indirect immunolabeling and western blotting. As seen in the Fig. 3 intense green color, mostly from the surface of MCF7 cells indicated the over-expression of folate receptor where as in folate receptor knockdown cells little or no green color was observed under fluorescence microscope. This study was further confirmed by western blotting (Fig.3 B, C) of cell lysate with antibody against folate receptor. From the figure 3A, it is seen that the expression of folate receptor was decreased significantly in FR<sup>-</sup> MCF7 cells compare to control cells.

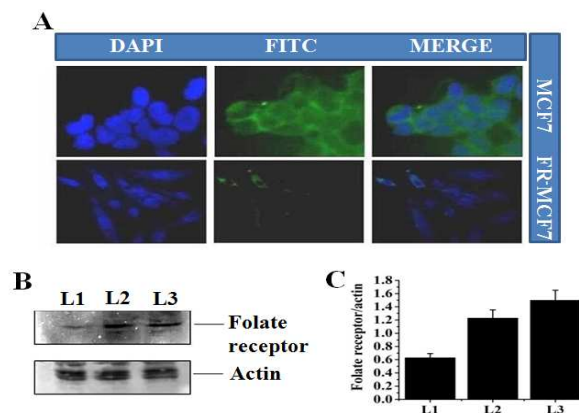
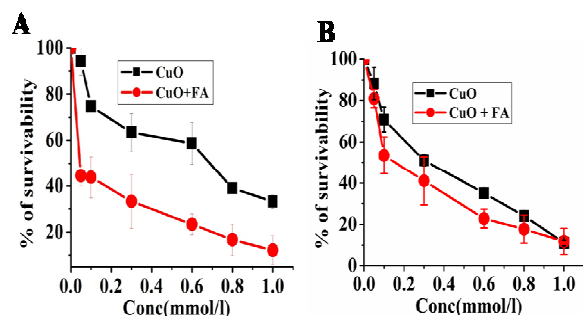


Figure 3: Expression of folate receptor in MCF7 cells,  $\alpha$  FR sh RNA transfected MCF7 cells (FR<sup>-</sup>MCF7) and scrambled sh RNA transfected MCF7 cells, (A) indirect immunolabeling with antibody against folate receptor. (B) Western blotting of cell extract with antibody against folate receptor: L1:FR<sup>-</sup>MCF7, L2: scrambled Sh RNA transfected MCF7 cells. L3: MCF7 cells. (C) Quantification of western blot.

### 2.3 Cytotoxicity assay

A concentration dependent study was conducted to find out the effects of CuO and CuO-FA NPs on MCF7 cells and FR<sup>-</sup> MCF7 cells. From the Fig. 4A, it was seen that the survivability of MCF7 cells were reduced to 33.27% and 12.25 % at the highest concentrations of CuO NPs and CuO-FA NPs respectively (  $1\text{ mmol/l}$ ). For FR<sup>-</sup> MCF7 cells, it was seen that the cell survivability was reduced to 11.12% and 11.32% at the highest concentration of CuO NPs and CuO-FA NPs respectively (Fig. 4B).  $LD_{50}$  values of CuO and CuO-FA NPs treated cells was also represented in Table 3.



**Figure 4:** Cell survivability of (A) MCF7 cells (B) FR-MCF7 cells treated with different concentration of CuO and CuO-FA NPs (0.05, 0.1, 0.3, 0.6, 0.8, 1 mmol/l).

**Table 3:** LD<sub>50</sub> doses of CuO and CuO-FA NPs

PARTICLE	MCF7	FR-MCF7
CuONPs	0.6mmol/l	0.4 mmol/l
CuO-FA NPs	0.1mmol/l	0.3 mmol/l

## 2.4 Reactive oxygen species (ROS) study

CuO and CuO-FA NPs induced oxidative stress was also examined in both MCF7 and FR-MCF7 cells. From the Fig. 5, it was seen that the difference of ROS production by CuO NPs was much higher in MCF7 cells compared to CuO-FA NPs treated MCF7 cells. In MCF7 cells, almost 1.6 fold ROS increased when treated with CuO-FA NPs compare to CuO NPs treated cells whereas in FR-MCF7 cells ROS production was almost same for CuO and CuO-FA NPs treated cells.

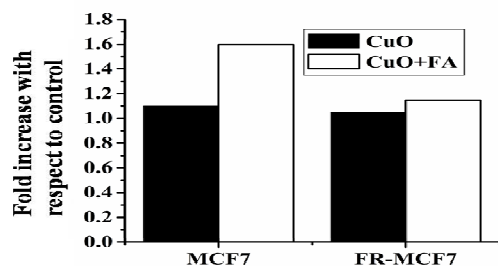


**Figure 5:** Measurement of ROS in CuO and CuO-FA NPs treated cell MCF7 and FR-MCF7 at their respective LD<sub>50</sub> value.

## 2.5 Apoptosis study by Annexin V-FITC staining

We next tried to estimate the apoptosis by AnnexinV-FITC staining after incubating the cells with CuO or CuO-FA NPs at LD<sub>50</sub> doses for 24 hrs. From the Fig. 6, it was seen that in untreated control group, very little amount of apoptotic cells present (4%), where as almost 19% and 62% cell death occur in case of CuO and CuO-FA NPs treated cells respectively. But in case of FR-MCF7 cells there is very little difference between CuO and CuO-FA NPs treatment. For FR-MCF7 cells, 8.4% and 16.9% apoptotic cells was observed in CuO and CuO-FA NPs treated cells respectively.

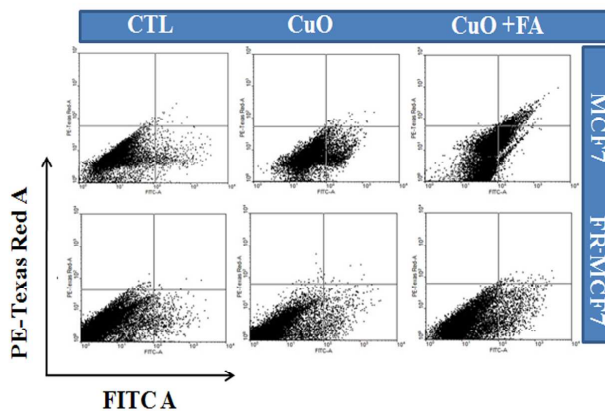


**Figure 6:** Apoptosis study by AnnexinV-FITC/PI staining of MCF7 and FR-MCF7. The lower left quadrants of each panels show the viable cells, which exclude PI and are negative for FITC-AnnexinV binding. The upper right quadrants contain the non-viable dead, positive for FITC-AnnexinV binding and for PI uptake. The lower right quadrants represent the apoptotic cells, FITC-AnnexinV positive and PI negative demonstrating cytoplasmic membrane integrity.

## 2.6 Cell cycle analysis by PI staining

Generation of ROS induced apoptosis is particularly support the sub G<sub>0</sub> peaks in the cell cycle analysis by FACS. We have analyzed the cell cycle of CuO and CuO-FA NPs treated MCF7 cells. From the Fig. 7, it is seen that SubG<sub>0</sub> population was almost 37% in case CuO-FA NPs treated cells where as only 22% for CuO NPs treated cells and very little amount (almost 4%) was found in control (CTL) cells.

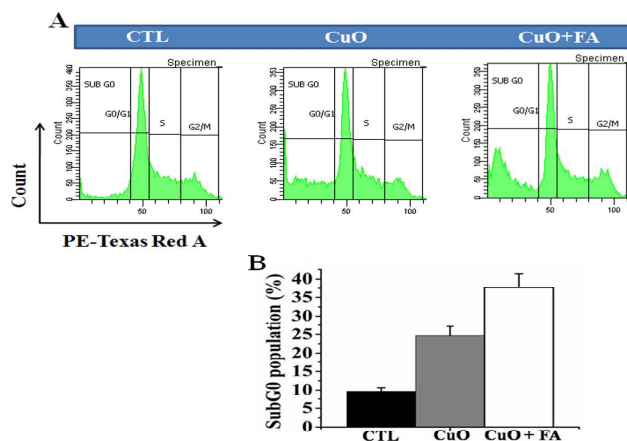


**Figure 7:** (A) Cell cycle analysis of CuO and CuO-FA NPs treated MCF7 cells at their respective LD<sub>50</sub> (B) quantification analysis of SubG0 population in CuO and CuO-FA NPs treated MCF7 cells.

### 2.7 Western blot analysis: expression of apoptotic protein

Western blot analysis was performed to further assess the apoptotic proteins (p-BAD and cleaved PARP) in CuO and CuO-FA NPs treated MCF7 and FR MCF7 cells. As seen in the Fig. 8 reduce expression of p-BAD indicates apoptosis in CuO-FA NPs treated cells. Cleaved PARP in CuO or CuO-FA NPs treated cells also observed.  $\beta$ -actin used as a loading control (Fig. 8).

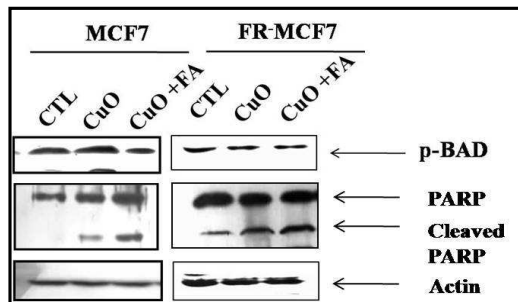


**Figure 8:** Western blot analysis of MCF7 and FR MCF7 cell extracts for p-BAD and PARP after exposure of cells with CuO NPs or CuO-FA NPs for 24 hrs.  $\beta$ -Actin was used as loading control.

### 2.8 In vivo therapeutic efficiency of folic acid modified CuO NPs

After induction of tumor by DL cells for 15 days, we isolated DL cell from tumor bearing mice and estimated some important parameters such as GSH, ROS, SGOT.

#### 2.8.1 Measurement of reactive oxygen species

The DL cells were collected from untreated, CuO NPs or CuO-FA NPs treated tumor bearing mice. Then, the ROS was estimated in these DL cells. ROS produced in DL cells was significantly increased (almost two fold) in case CuO-FA NPs treated mice, whereas very little amount increased in CuO NPs treated tumor bearing mice (Table 4).

#### 2.8.2 Measurement of intracellular glutathione

As oxidative stress increased, among different biological changes occur inside the cells, anti-oxidant enzymes glutathione is also deplete. Thus, we measured the total GSH content of the cells isolated from tumor. It is seen that the GSH content of CuO-FA NPs treated cells was decreased more compare to CuO NPs treated cells or control cells (Table 4).

#### 2.8.3 Measurement of serum glutamic oxaloacetic transaminase (SGOT)

In addition, the toxicity of all mice was monitored by serum chemistry examinations. The SGOT level of CuO NPs treated mice was not significantly changed after 10 days of exposure, while the level significantly increased after 15 days of exposure where as in case of CuO-FA NPs, SGOT level increased slightly during the same time interval. These results indicated that liver inflammation might be induced in CuO NPs treated mice after 10 days, which was reduced in CuO-FA NPs treated mice as seen in Table 4.

**Table 4:** Measurement of ROS, GSH, SGOT of DL cells isolated from mice.

Assay	CTL			CuO NPs			CuO-FA NPs		
ROS fold increase (A.U)	1			1.2			1		
GSH ( $\mu$ g/ml)	22 $\pm$ 1.22			12 $\pm$ 1.12			7 $\pm$ 0.67		
SGOT(IU/Lit) days	3	5	10	3	5	10	3	5	10
	6.5	6.9	6	10	11.5	26.1	8.5	10	13

#### 2.8.4 Apoptotic morphological changes by AO/ Et-Br staining

CuO and CuO-FA NPs induced apoptosis or necrosis was examined in DL cells using acridine orange and ethidium bromide dual staining. Viable cells took the green color of acridine orange with normal cell morphology as seen in control cells. Acridine orange and ethidium bromide stained cells with condensed nucleus were found in CuO-FA NPs treated mice (Fig. 9) indicating early or late apoptosis stages where as some necrotic cells (red) were present in CuO NPs treated mice.



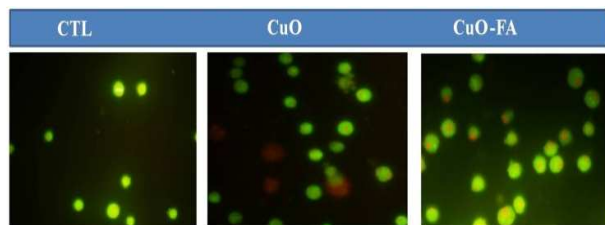


**Figure 9:** Qualitative characterization nuclear morphology by EtBr/AO staining.

### 2.8.5 MTT assay: Viability analysis of DL cells

Viability analysis of DL cells of peritoneal fluid revealed that both CuO and CuO-FA NPs treatment in tumor-bearing mice led to a significant reduction in the number of malignant cells compare to the control group. From the Fig. 10 B, it is seen that 58% of the cells survived in CuO NPs treated mice, where as 25% cells survived for CuO-FA NPs treated mice.

### 2.8.6 Effect of CuO NPs and CuO-FA NPs on tumor volume and days of survivability

Administration of CuO and CuO-FA NPs extended the life span of tumor bearing mice. From the first day of tumor induction, we found that the untreated tumor control mice survived for only 13 days which was extended up to 19 days and 29 days for CuO NPs and CuO-FA NPs treated tumor bearing mice respectively (Fig. 10B). The tumor volume in the control mice was about 8.3 ml, it was significantly reduced to 5.4 ml and 3.3 ml in the group 3 and group 4 mice respectively at a concentration of 8 mmole/l/Kg BW (3days) for 15 days (Fig.10 C). Cell survivability was also decreased in case of CuO-FA NPs treated mice (Fig. 10 D).

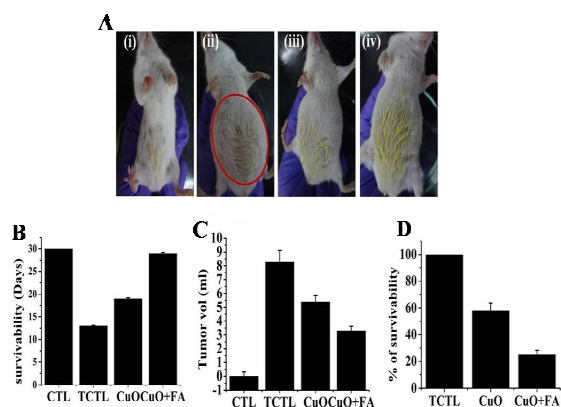


**Figure 10:** (A) Pictorial representation of (i) normal mice; (ii) DL cell induced tumor mice (TCTL); (iii) DL cell induced tumor mice treated with CuO NPs and (iv) DL cell induced tumor mice CuO-FA NPs. Red circle indicates the development of tumor in TCTL mice. (B) Measurement of tumor volume in normal mice; DL induced tumor mice; DL induced tumor mice treated with CuO and CuO-FA NPs. (C) Survivability test of mice (D) Viability of tumor cells isolated from DL tumor bearing mice.

### 2.9 Discussion

Recently, numerous metal based nanoparticles have been proposed for therapeutic purpose which can replace the expensive chemotherapeutic drug. The greatest challenge in this regard is to confine the activity of nanoparticles to tumor mass. The cytotoxic effect of CuO NPs has been shown in number of studies but has yet to be optimized for effective delivery of these nanoparticles for therapeutic applications. In this study, we have tried to deliver CuO NPs through folic acid in in vitro and in vivo model. Toxicity of CuO NPs in different cells has been reported earlier.<sup>15,16</sup> In our previous study, we have also seen CuO-NPs induce cell death by autophagy.<sup>17</sup> Among the different approaches to target cancer cells FA is one of the targeting agents which can be manipulated easily and moreover it is cost effective. Additionally, folate receptor has been frequently over-expressed in many types of cancer and normal cells express none or very few folate receptors. The folate receptor distribution in various tissues is discussed in detail by Weitman et al., 1992.<sup>18</sup> Zhang et al., already delivered FA modified gold nanoparticles for targeted therapy in Hela cell.<sup>19</sup> Here, FA is conjugated with CuO-NPs by three-steps through surface modification of CuO NPs. The APTS can be easily attached to the surface of CuO NPs to form stable CuO-NH<sub>2</sub>. DCC and NHS are used to activate the carboxyl groups of FA, forming a highly reactive intermediate (NHS-carboxylate). Zhang et al., also used APTS to functionalize magnetic nanoparticle for in vivo delivery.<sup>20</sup> One step further, we have also conjugated FA with amine functionalized CuO NPs for targeted delivery. DLS size also showed that the size of CuO-FA NPs much more higher than CuO NPs and FESEM image also revealed that pure CuO NPs are almost spherical geometry but after conjugation some agglomerated particles are also present. The conjugation was further confirmed by FTIR study. In our

experiment, MCF7 cells were taken as target cells while FR<sup>-</sup> MCF7 cells lack of folate receptors, were used as control cells. Although, the toxicity of CuO NPs is well known compared to other metal oxide NPs, but CuO NPs can be easily manipulated to attach with targeting ligand and also their production cost is less. So, we have tried to deliver CuO NPs through folic acid, where FRs are often over-expressed in cancer cells. First, we have seen the cytotoxic effect of CuO and CuO-FA NPs on in vitro system. From the cell survivability assay, it is seen that CuO-FA NPs is more active on MCF7 cells as folate receptors are over expressed in MCF7 cells.<sup>21</sup> While knocking down of folate receptor in the isogenic cells showed less toxic effect when treated with CuO-FA NPs. Also, almost no difference in toxicity induced by CuO and CuO-FA NPs in folate receptor knock down MCF7 cells were observed (compare the LD<sub>50</sub> values). Thus, the amount of ROS production in MCF7 cells was much more higher than folate receptor knock down cells, indicating more CuO NPs were uptaken by folate receptor positive MCF7 cells. Consequently, enhanced ROS generation explained the induction of apoptosis in MCF7 cells when treated with CuO-FA NPs compare to folate receptor knock down MCF7 cells. Additionally, we have also estimated the apoptotic cells by annexinV-FITC staining. ROS generation was increased in CuO-FA NPs treated cells, from the flow cytometric analysis we have also got more annexinV-FITC positive cells in case CuO-FA NPs treated cells. Extract from CuO and CuO-FA NPs treated cells was immunoblotted with p-BAD and PARP antibody. Also p-BAD more decreased and cleaved PARP increased significantly which indicated more apoptotic cells in CuO-FA NPs treated MCF7 cells. Thus, CuO-FA NPs may be used as a therapeutic purpose. For this approach, we have studied the therapeutic efficacy of CuO and CuO-FA NPs in intracavitary peritoneal tumor model.

#### **In vivo therapeutic efficiency of CuO and CuO-FA NPs**

For in vivo therapeutic efficiency, we have developed tumor bearing mice after intracavitary peritoneal inoculation of DL cells. With the time, the tumor volume was increased significantly in the control mice. Initially in normal mice, the optimum doses of CuO NPs was estimated and the same was used for the experiments. The folate receptor is over-expressed in a broad spectrum of malignant tumors and represents an attractive target for selective delivery of anticancer agents to folate receptor-expressing tumors. DL cells, also over-expressed folate receptor and thus treatment of mice with CuO-FA NPs facilitate the reduction of tumor size and extended the life span of the tumor bearing mice.<sup>29</sup> Also, when the cells isolated from tumor, the percentage of live cells were decreased significantly for

the group of mice treated with CuO-FA NPs as comparable to CuO NPs treated group and most of the cell death were apoptosis which was also observed in our in vitro experiments with MCF7 cells. Nevertheless, SGOT, the serum parameter for estimating liver damage were not increased upto 10 days in CuO-FA NPs treated group. But in the non-targeted group, which was treated with CuO NPs, SGOT level increased remarkably after 10 days indicating the toxic effect of CuO NPs. Similarly, the level of ROS increased and GSH decreased in the tumor cells when the mice was treated with CuO-FA NPs. Decreased of total GSH indicated the enhancement of oxidative stress induced by CuO-FA NPs, inside the tumor. In non targeted group treated with CuO NPs, the generation of ROS and reduction of GSH level in the tumor cells did not increased, suggesting less cytotoxic effect. As a matter of fact, reduced life span and slightly reduced tumor volume of this group of mice indicated other toxicity induced by CuO NPs. At the same time, CuO-FA NPs efficiently reduced the tumor volume and increased the tumor cells death compared to non-targeted group. Thus, the cytotoxic effect of CuO-NPs is confined to the folate receptor expressing tumor cells indicating CuO-FA NPs could potentially target the tumor cells. Thus, CuO-FA NPs was successfully delivered to the tumor and the cytotoxicity of the normal cells can be avoided. Moreover, this technique can be exploited to target other cancer cell surface specific markers for the development of cost effective chemotherapeutic drug.

### **3. Experimental Section**

#### **3.1 Chemical reagents**

Copper acetate, sodium hydroxide and acetic acid were obtained from Merck (Germany). 3-(4,5-dimethylthiazol-2-yl)-2,5-diphenyltetrazolium bromide (MTT) and Folic acid were obtained from SRL (India). Bovine serum albumin (BSA), 3-Aminopropyl trimethoxy silane (APTS), N-Hydroxysuccinimide (NHS) and 1-Ethyl-3-(3-dimethylaminopropyl)carbodiimide (EDC) were purchased from sigma (USA). 4',6-diamidino-2-phenylindole (DAPI) was obtained from Vector Laboratories (USA). Horseradish peroxidase (HRP) conjugated secondary antibodies, Anti FR goat polyclonal IgG,  $\alpha$  FR sh RNA (SC-39969) lentiviral particles were obtained from Santa Cruz Biotechnology (USA).

#### **3.2 Synthesis of Copper oxide nanoparticles**

We have synthesized CuO NPs according our previous protocol.<sup>17</sup> In brief, copper acetate [Cu(CH<sub>3</sub>COO)<sub>2</sub>] was dissolved in de-ionized water followed by the addition of 50 mM of acetic acid under



stirring condition. The solution was heated at boiling temperature at 78 °C. 100 mM of NaOH was added directly to the above solution under vigorous stirring. The reaction was performed for 1 hrs. Resultant product was collected by centrifugation. Finally, it was dried at room temperature.

### 3.3 Amine functionalized of Copper oxide nanoparticles

Surface modification of CuO NPs was done by 3-Aminopropyltrimethoxy silane (APTS). In brief, about 200 mg of CuO NPs was dispersed in about 100 ml of DMSO in a sonication bath for about 1 hrs and then 400µl of APTS was drop wise added under heating condition. These amine functionalized CuO NPs (CuO-NH<sub>2</sub>) was collected by centrifugation process and washed with de-ionized water.<sup>23</sup>

### 3.4 Chemical activation of folic acid and conjugation with CuO-NH<sub>2</sub>

The carboxyl group (-COOH) of FA was activated by EDC/NHS. In brief, FA was dissolved in DMSO. After that, EDC/NHS was added to the above solution for activation of FA. The activated FA was added drop wise in CuO-NH<sub>2</sub> solution. The FA modified CuO NPs was obtained by centrifugation of the reaction mixture at 10 000 rpm for about 15 mins and washed for few times. Finally, these were dried by freeze dried.

### 3.5 Physical characterization of CuO and FA modified CuO NPs

Physical characterization was done by DLS, Zeta-potential, FESEM, FTIR. Briefly, CuO and CuO-FA NPs was dispersed in milliQ using sonicator for 1hrs for 0.5mg/ml. The particle size and zeta potential was measured Brookhaven 90 plus particle size analyzer (DLS). The surface morphology of the nanoparticles was analyzed by field emission scanning electron microscopy (FESEM) with Phillips CM 200 microscope. The average particle size from FESEM micrographs was analyzed using image J software. The surface composition of the nanoparticles at each step of surface modification was determined from FTIR spectra. Samples for FTIR spectra were prepared in KBr in the range 4000-400 cm<sup>-1</sup>.

### 3.6 Cell culture and treatments

Human breast cancer cells MCF7 was purchased from National Centre for Cell Science (Pune, India) and cultured in RPMI-1640 media supplemented with 10% FBS and 100 U ml<sup>-1</sup> penicillin–streptomycin at 5% CO<sub>2</sub> and 37 °C. At 85% confluence, cells were harvested and sub-cultured according to experimental requirements. Cells were seeded for 24 hrs prior to the treatment with CuO NPs

and CuO-FA NPs. All the treatments were performed at 37 °C at a density allowing experimental growth.

### 3.7 Small hairpin RNA (sh RNA) mediated silencing of Folate receptor (FR)

MCF7 cells were transfected with α FR sh RNA or scramble sh RNA using Santa Cruz transfection reagent according to the manufacturer's instructions. Briefly, cells were seeded in 35mm for 18 hrs. After that, cells were transfected with α FR shRNA or scrambled sh RNA lentiviral particle for 6 hrs. Then, the medium was changed and incubated additional 18hrs. Finally, knockdown efficacy of these cells was determined by western blotting and immune-fluorescence microscopy with anti- FR antibody.

### 3.8 Receptor expression by Immunofluorescence microscopy

Knockdown efficacy was determined by Immunofluorescence technique.<sup>24</sup> Briefly, both MCF7 cells and FR<sup>-</sup>MCF7 cells were plated on 18 mm glass cover slips. After 24hrs incubation in complete medium, cells were fixed in freshly prepared 4% paraformaldehyde solution for 15 min and permeabilized with 0.2% Triton X-100 on ice for 10 min. The fixed cells were pre-incubated in blocking solution (1% BSA in 1× PBS), followed by overnight incubation with anti-FA antibody (Santa Cruz Biotechnology, USA; 1:100) in wash buffer (0.1% BSA and 0.05% Tween 20 in 1× PBS) at 4 °C. Cells were then washed three times with wash buffer and probed with fluorescein isothiocyanate (FITC) conjugated anti-mouse antibody (Molecular Probes, USA; 1:500) for 1 hrs at RT. After washing, cells were mounted in the mounting solution containing DAPI and examined under a fluorescence microscope (Leica, Germany).

### 3.9 Cell viability: MTT assay

The inhibition of cell growth was measured by MTT assay as described previously.<sup>25</sup> Briefly, cells were seeded in 24 well plates at a density of 1 × 10<sup>4</sup> cells per well and exposed to CuO or CuO-FA NPs at different concentrations ( 0.05, 0.1,0.3, 0.6 ,0.8, 1 mmole/l/kg) for 24 hrs. After that, the culture media was discarded and incubated with MTT solution (450µg/ml) for 3-4 hrs at 37 °C. The resulting formazan crystals were dissolved in a MTT solubilization buffer and the absorbance was measured at 570 nm by using a micro plate reader (Biotek, USA). Each point was assessed in triplicate manner.

### 3.10 Detection of intracellular reactive oxygen species (ROS) levels

For quantifying the intracellular ROS, both MCF7 cells and FR<sup>-</sup>MCF7 cells were seeded in 60 mm plate. Briefly, 5 × 10<sup>5</sup> cells were

treated with CuO and CuO-FA NPs on both cells at their respective median lethal doses ( $LD_{50}$ ) for 6 hrs and harvested. Then, DCFDA (20 mM) was added to the cell suspension and kept for 30 min at 37 °C. DCFDA diffuses through the cell membrane, enzymatically hydrolysed by intracellular esterases and oxidized to produce a fluorescent 2', 7'- dichlorofluorescein (DCF) in the presence of ROS. The intensity of fluorescence is measured at 529 nm by spectrofluorimeter (Epoch, USA). The intensity of fluorescence is proportional to the level of intracellular reactive oxygen species.<sup>15</sup>

### 3.11 Measurement of Apoptotic cells: AnnexinV-FITC staining

In this study,  $1 \times 10^6$  cells/ml suspensions of human breast cancer cells MCF7 cells and FR-MCF7 cells were induced for apoptosis by addition of  $LD_{50}$  doses of CuO or CuO-FA NPs respectively and untreated cells were kept as control. Both control and test samples were incubated for 24 hrs in a 37 °C, 5% CO<sub>2</sub> incubator. Following the incubation, the cells were washed twice with  $1 \times$  PBS. After that, the cells at concentration of about  $1 \times 10^6$  cells/ml were re-suspended in  $1 \times$  Annexin binding buffer. 500  $\mu$ l of each cell suspension was added to a plastic 12  $\times$  75 mm FACS tube and 2  $\mu$ g/ml of AnnexinV-FITC (Invitrogen) and 0.5  $\mu$ g/ml of propidium iodide (Invitrogen) were added to each cell suspension. Then, the tubes were incubated at room temperature for exactly 15 min at dark condition.<sup>26</sup>

### 3.12 Cell cycle analysis

For cell cycle analysis,  $1 \times 10^6$  cells/ml were treated with CuO NPs or CuO-FA NPs at  $LD_{50}$  dose. After 24 hrs incubation, the cells were washed with  $1 \times$  PBS and fixed with chilled 80% ethanol and kept for 2 hrs at 4 °C. Prior to stain with 50  $\mu$ g/ml propidium iodide (PI, Sigma), the cells were incubated for 1 hrs with 100  $\mu$ g/ml of DNase free RNase A (SRL, India) at 37 °C. The cell cycle was analyzed with a Becton Dickinson (FACS Calibur) flow cytometer, equipped with an air-cooled 20 mW argon laser. 25,000 events were counted at each data point.

### 3.13 Western blot assay

The cell extract of CuO NPs and CuO-FA NPs treated cells (MCF7 and FR-MCF7) was determined by western blot. Cells were treated with appropriate time at  $LD_{50}$  dose. After that, cells were lysed using RIPA buffer. The supernatants were collected as cell lysates and protein concentrations were normalized, after determining protein concentrations by the Bradford assay and followed by SDS-gel electrophoresis. Whole cell lysates with equal protein amounts

were loaded in each lane and separated on a 10% SDS-PAGE gel. The proteins on the gels were then transferred to nitrocellulose membranes and nonspecific binding sites were blocked by incubation in BSA for 1 hrs. Then, blots were probed with primary antibodies (PARP, p-BAD) for overnight at 4 °C. Subsequently, the membrane was incubated with appropriate secondary anti-rabbit antibodies conjugated with horseradish peroxidase. The membrane was then incubated with enhanced chemiluminescence reagent (ECL) solution for 3 min. Visualization of the immune-labelled bands was carried out by auto-radiography.<sup>27</sup> To confirm equal protein loading in each lane, membranes were re-probed with  $\beta$ -actin antibody (1:5000 dilution).

## In vivo experiment

### 3.13 Animals

Swiss mice aged 6–8 weeks old, weighing about 25–30 g, were used in the experiments. The animals were fed a standard pellet diet with vitamins and water ad libitum and housed in a polypropylene cage (Tarson, India) in the departmental animal house with a 12 hrs light: dark cycle under a standard temperature. The animals were allowed to acclimatize for 1 week. The animals did not show any pathological symptoms. Animals were maintained in accordance with the guideline of the National Institute of Nutrition, Hyderabad, India, Indian Council of Medical Research and approved by the ethical committee of Vidyasagar University.

### 3.14 Development of In vivo Tumor

Dalton lymphoma (DL) was induced by intra-peritoneal (i.p.) serial transplantations of  $1 \times 10^7$  viable tumor cells (assayed by the trypan blue method) per mice with 100% success each time. Development of DL was confirmed by abnormal belly swelling and increased body weight, which were visible in 10–12 days of implantation.<sup>28</sup>

### 3.15 Experimental design In vivo

Initially, we have screened the dosage of 4, 8, 16, 32 mmol/l/Kg of CuO and CuO-FA NPs of in-vivo treatment. We have seen that in case of 8 mmol/l/Kg for CuO and CuO-FA NPs treated mice were healthy and the tumor was reduced.

The mice were randomly divided into four groups, with three animals in each group:

- Group 1: blank non-tumor mice (non-tumor and untreated)
- Group 2: tumor control mice (tumor induced and untreated)
- Group 3: tumor-induced mice (treated with 8 mmole/l/Kg CuO NPs)

Group 4: tumor-induced mice (treated with 8 mmol/l/Kg CuO - FA NPs)

### 3.16 Euthanasia of Experimental Animals

After completion of the experimental treatment, all the mice were deprived of food overnight and euthanized by cervical dislocation under ketamine-xylazine anaesthesia. The ascetic fluid was collected carefully for different types of estimations.

### 3.17 Measurement of ROS generation

Procedure for ROS measurement as mention in in vitro section for MCF7 cells. We have used the same protocol for determination of ROS of Dalton lymphoma cell isolated from tumor bearing mice. In summary, we isolated the Dalton lymphoma cells from CuO and CuO-FA NPs treated mice and untreated tumor bearing mice and the ROS was measured followed by above protocol.

### 3.18 Analysis of intracellular glutathione

DL cells of peritoneal fluid were isolated from untreated, CuO and CuO-FA NPs treated mice. These cells were washed with PBS and 1000 $\mu$ l of ice-cold 5% (w/v) sulphosalicylic acid (SSA) was added to the above cells. The lysate was incubated for 15min at -20°C and then thawed on 37° C water bath for 10min. This step was repeated thrice. Cold centrifugation was carried out at 8000 rpm for 5min at 4°C. Then to each cell lysate 50 $\mu$ l DTNB, 100 $\mu$ L of 1M Tris Cl pH-8.0 and 840 $\mu$ l of double distilled water. The solution was mixed properly and O.D. was taken at 412nm.

### 3.19 Serum chemistry studies for liver function

At first, the mice were anesthetized and blood samples were collected by intra cardiac puncture using a spectrofluorimeter syringe after 3, 5 and 15 days. Then, the plasma samples were obtained by centrifugation (6000 rpm, 10 min) of the blood and the levels of serum glutamic oxaloacetic transaminase (SGOT) were measured according to standard method.<sup>29</sup>

### 3.20 Apoptosis and Necrosis study by AO/EB staining

The DL cells were isolated from untreated and treated mice (CuO and CuO-FA NPs) and stained with AO/EB (Sigma-Aldrich) dual dye in order to detect apoptotic or necrotic nuclei. A solution of PBS containing EtBr and AO (50  $\mu$ g/ml; V/V) was added to the cell suspension. Living cells stained with green (AO). Only cells that had membrane pores or cells that had ruptured allowed the diffusion of EtBr into the cell cytosol. Images were acquired using an inverted fluorescence microscope with an original magnification of 40X.<sup>29</sup>

### 3.21 Effect of nanoparticles on ascetic tumor

The MTT assay was used for the in vivo experiments. Tumor mice in Group 3 were treated with CuO NPs, Group 4 treated with CuO-FA NPs at a different concentration for a period of 15 days and their ability to reduce tumor volume and the number of cells was compared with Group 1 control mice and Group 2 tumor control mice.

## 4. Conclusions

In summary, we have successfully designed and synthesized FA modified CuO NPs. This was delivered in folate receptor positive breast cancer MCF7 cells as well as DL tumor bearing mice model. The uptake of CuO-FA NPs was higher than that equivalent dose of CuO NPs in both folate receptor positive MCF7 cells also in DL tumor bearing mice. These result strongly suggested that CuO NPs can be used as a therapeutic purpose through folic acid mediated delivery. The application of this targeted delivery tested on more animal model and also the application in vivo is limited to the cancer.

## Acknowledgements

The authors would like acknowledge to Department of Biotechnology, Government of India (No-BT/PR14661/NNT/28/494/2010) for financial support for this research work.

## References

1. P. Kumar, N. B. Bolshette, V. S. Jamdade, N. A. Mundhe, K. K. Thakur, K. K. Saikia, M. Lahkar. Breast cancer status in India: An overview. *Biomedicine & Preventive Nutrition*. 2013, **3**, 177-183.
2. A. Surendiran, S. Sandhiya, S.C. Pradhan and C. Adithan Novel applications of nanotechnology in medicine. *Indian J. Med. Res.* 2009,**130**, 689-701.
3. R. Coradeghini, S. Gioria, C. Pascual Garcia, P. Nativo, F. Franchini, D.Gilliland, J. Ponti and F. Rois. Size-dependent toxicity

and cell interaction mechanisms of gold nanoparticles on mouse fibroblasts. *Toxicol. Lett.* 2013, **217**, 205-216.

4.Y. Zhang, D.Xu, W. Li, J. Yu and Y.Chen Effect of Size, Shape, and Surface Modification on Cytotoxicity of Gold Nanoparticles to Human HEP-2 and Canine MDCK Cells. *J. Nano Mat.* 2012, doi:10.1155/2012/375496

5.A. Sarkar, M. Ghosh, P. C. Sil, Nanotoxicity: Oxidative Stress Mediated Toxicity of Metal and Metal Oxide Nanoparticles. *J. Nanosci. Nanotechnol.* 2014, **14**, 730-743.

6. B. Sha, W. Gao, S. Wang, X. Gou, W. Li, X. Liang, Z. Qu, F. Xu, T.J. Lu Oxidative stress increased hepatotoxicity induced by nano-titanium dioxide in BRL-3A cells and Sprague-Dawley rats. *J. Appl. Toxicol.* 2014, **34**, 345-56.

7. J. Kim, H. Kim, S. S. A An2, H.Maeng, M.Kim, Y. Song In vitro cytotoxicity of SiO<sub>2</sub> or ZnO nanoparticles with different sizes and surface charges on U373MG human glioblastoma cell. *Int. J. Nanomedicine.* 2014, **9**, 235-241.

9. S. D. Bucchianico, M. R. Fabbrizi, S. K. Misra, E. Valsami-Jones, D. Berhanu, P. Reip, E.Bergamaschi and L. Migliore, Multiple cytotoxic and genotoxic effects induced in vitro by differently shaped copper oxide nanomaterials. *Mutagenesis.* 2013, **28**, 287-299.

10. D. Laha, D. Bhattacharya, A. Pramanik, C. R. Santra, P. Pramanik and P. Karmakar. Evaluation of copper iodide and copper phosphate nanoparticles for their potential cytotoxic effect. *Toxicol. Res.* 2012,**1**,131.

11.T. Mironava M. Simon, M. H. Rafailovich, B. Rigas, Platinum folate nanoparticles toxicity: Cancer vs. normal cells. *Toxicol. in Vitro.* 2013, **27**, 882-889.

12.C. Haglund, A. A. leskog, P. Nygren, J. Gullbo, M.H. glund, M. Wickstrom, R. Larsson and E. Lindhagen. In vitro evaluation of clinical activity and toxicity of anticancer drugs using tumor cells from patients and cells representing normal tissues. *Cancer Chemother. Pharmacol.* 2012, **69**, 697-707.

13.T. Muthukumar, M. Chamundeeswari, S. Prabhavathi, B. Gurunathan, J. Chandhuru and T. P. Sastry. Carbon nanoparticle from a natural source fabricated for folate receptor targeting, imaging and drug delivery application in A549 lung cancer cells. *Eur. J. Pharm. Biopharm.* 2014, **88**, 730-736.

14. S. Pandey, G. Oza, A. Mewada, R. Shah, M. Thakur and M. Sharon. Folic acid mediated synaphic delivery of doxorubicin using biogenic gold nanoparticles anchored to biological linkers. *J. Mater. Chem. B*, 2013, **1**, 1361.

15. B. Fahmy, S. A. Cormier. Copper oxide nanoparticles induce oxidative stress and cytotoxicity in airway epithelial cells. *Toxicol. in Vitro.* 2009, **23**,1365-1371.

16.A. M. Studer, L. K. Limbach, L. V. Duc, F. Krumeich, E. K. Athanassiou, L.C. Gerber, Holger Mochb, Wendelin J. Stark. Nanoparticle cytotoxicity depends on intracellular solubility: Comparison of stabilized copper metal and degradable copper oxide nanoparticles. *Toxicol. Lett.* 2010, **197**, 169-174.

17. D. Laha, A. Pramanik, J. Maity, A. Mukherjee, P. Pramanik, A. Laskar, P. Karmakar. Interplay between autophagy and apoptosis mediated by copper oxidenanoparticles in human breast cancer cells MCF7. *Biochimica et Biophysica Acta.* 1840, **2014**,1-9.

18. S.D. Weitman, R.H. Lark, L.R. Coney, D.W. Fort, V. Frasca, V.R. Zurawski, B.A. Kamen. Distribution of the folate receptor GP38 in normal and malignant cell lines and tissues. *Cancer Res.* 1992, **12**, 3396-401.

19. Y. Zhang, D. Xu, W. Li, J. Yu, and Y. Chen. Effect of Size, Shape, and Surface Modification on Cytotoxicity of Gold Nanoparticles to Human HEP-2 and Canine MDCK Cells. *J. Nano Mat.* 2012. doi:10.1155/2012/375496.

20. F. M. Kievit and M. Zhang. Surface Engineering of Iron Oxide Nanoparticles for Targeted Cancer Therapy. *Acc. Chem. Res.* 2011,**44**, 853-862.

21.H. Banu, B. Stanley, S. M. Faheem, R. Seenivasan, K. Premkumar and G.Vasanthakumar. Thermal Chemosensitization of Breast Cancer Cells to Cyclophosphamide Treatment Using Folate Receptor Targeted Gold Nanoparticles. *Plasmonics*, 2014, **9**,1341-1349.

22. H. Shmeeda, L. Mak, D. Tzemach, P. Astrahan, M. Tarshish and A. Gabizon. Intracellular uptake and intracavitary targeting of folate conjugated liposomes in a mouse lymphoma model with up-regulated folate receptors. *Mol. Cancer Ther.* 2006, **5**, 808-816.

23. S. Mitra, S. Chandra, D. laha, P. Patra, N. Debnath, A. Pramanik, P. Pramanik, A. Goswami. Unique chemical grafting of carbon nanoparticle on fabricated ZnO nanorod: Antibacterial and bioimaging property. *Materials Research Bulletin*, 2012, **3**, 586-594.

24. A. Mukherjee, S. Samanta, P. Karmakar. Inactivation of PTEN is responsible for the survival of Hep G2 cells in response to etoposide-induced damage. *Mutation Research.* 2011,**715**, 42- 51.

25. Arindam Pramanik, Dipranjan Laha, Panchanan Pramanik, Parimal Karmakar. A novel drug "copper acetylacetonate" loaded in folic acid-tagged chitosan nanoparticle for efficient cancer cell targeting. *J. Drug Target.* 2014, **22**, 23-33.

26. S. S. Fard, M. Jeddi-Tehrani, M. Mehdi Akhondi, M. Hashemi, and A. M. Ardekani. Flow Cytometric Analysis of 4-HPR-induced Apoptosis and Cell Cycle Arrest in Acute Myelocytic Leukemia Cell Line (NB-4). *Avicenna. J. Med Biotechnol.* 2010, **2**, 53-61.

27. T. Mahmood and P. Yang. Western Blot: Technique, Theory, and Trouble Shooting. *N Am. J. Med. Sci.* 2012, **9**, 429- 434.

28. M. I. Sriram, S. B. M. Kanth, K. Kalishwaralal and S. Gurunathan. Antitumor activity of silver nanoparticles in Dalton's lymphoma ascites tumor model. *Int. J. Nanomedicine.* 2010, **5**, 753-762.

29. S. Chattopadhyay, S. K.Dash, S. Tripathy, B.Das, S. K. Mahapatra, P. Pramanik and S.Roy. Cobalt oxide nanoparticles induced oxidative stress linked to activation of TNF- $\alpha$ /caspase-8/p38-MAPK signaling in human leukemia cells. *J. Appl. Toxicol.* 2015, **35**, 603-613.

